

Using Single Quantum States as Spin Filters to Study Spin Polarization in Ferromagnets

Mandar M. Deshmukh and D. C. Ralph

Laboratory of Atomic and Solid State Physics, Cornell University, Ithaca, New York 14853

(Received 10 July 2002; published 12 December 2002)

By measuring electron tunneling between a ferromagnet and individual energy levels in an aluminum quantum dot, we show how spin-resolved quantum states can be used as filters to determine spin-dependent tunneling rates. We also observe magnetic-field-dependent shifts in the magnet's electrochemical potential relative to the dot's energy levels. The shifts vary between samples and are generally smaller than expected from the magnet's spin-polarized density of states. We suggest that they are affected by field-dependent charge redistribution at the magnetic interface.

DOI: 10.1103/PhysRevLett.89.266803

PACS numbers: 73.23.Hk, 75.50.Cc, 75.70.Cn

Quantum dots are useful for studying electron spins, because they allow individual spin-resolved states to be examined in detail. Previous experiments have probed spin physics within several types of quantum dots: semiconductors [1–4], nonmagnetic metals [5,6], carbon nanotubes [7], and ferromagnets [8]. Here we use the individual spin-resolved energy levels in a nonmagnetic quantum dot to investigate the physics of a bulk magnetic electrode. The spin polarization in the magnet affects electron tunneling via the dot levels in two ways. First, tunneling rates are different for spin-up and spin-down electrons; we demonstrate how the tunneling polarization can be measured by using quantum-dot states as spin filters [9]. Second, as a function of magnetic field, the electrochemical potential of the magnetic electrode shifts relative to the energy levels in the dot. Previously, tunneling polarizations [10] and electrochemical shifts [11] have been measured by other techniques in larger devices having continuous densities of electronic states. By probing at the level of single quantum states, we are able to compare both effects in one device. In comparison to [11], we also achieve more precise measurements of the electrochemical shifts [12], which allow us to demonstrate that they are not determined purely by the bulk properties of the magnet, as has been assumed previously [11,13].

Our quantum dot is an Al particle, 5–10 nm in diameter, connected by Al_2O_3 tunnel junctions to an Al electrode on one side and a cobalt or nickel electrode on the other (Fig. 1, inset). We use an Al particle to minimize spin-orbit coupling, so that electronic states within the particle are to a good approximation purely spin-up or spin-down [5,6]. Device fabrication is done following the recipe in [5], except that in the final step we deposit 80 nm of magnetic Co or Ni at a pressure of $\sim 2 \times 10^{-7}$ torr to form the second electrode. We conduct tunneling measurements in a dilution refrigerator, using filtered electrical lines that provide an electronic base temperature of approximately 40 mK. Beyond a threshold voltage determined by the charging energy, electron tunneling via individual quantum states in the Al particle produces discrete steps in the I - V curve [5] or equivalently peaks

in dI/dV vs V (Fig. 1). The sign of bias refers to the sign applied to the Al electrode. Figure 2 shows how the energy levels in the particle undergo Zeeman spin splitting as a function of magnetic field (B , applied in the plane of the nitride membrane) [5]. The Co-lead sample also exhibits nonlinearities for $B < 0.3$ T, possibly associated with magnetic-domain rotation.

Before we turn to our main results, we note some experimental details. In order to convert the measured voltages of the resonances to energy, one must correct for the capacitive division of V across the two tunnel junctions. For a tunneling transition across the nonmagnetic (N) junction, this is accomplished by multiplying V by $eC_F/(C_N + C_F)$ and for the ferromagnetic (F) junction by $eC_N/(C_N + C_F)$, where C_N and C_F are the two junction

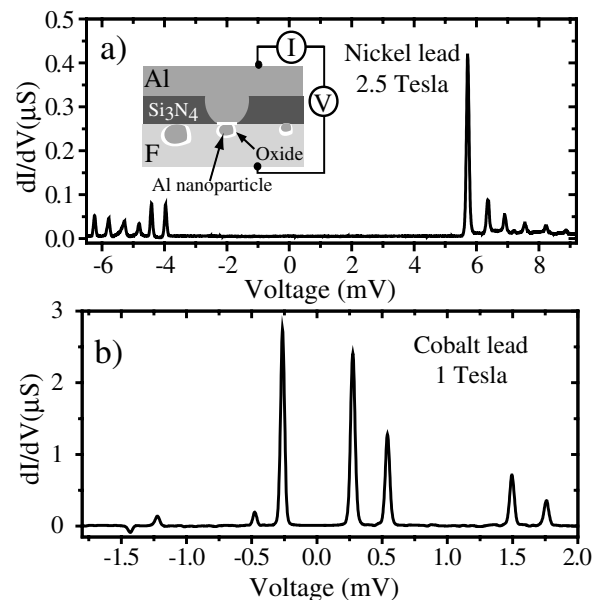


FIG. 1. (inset) Cross-sectional device schematic. (a) Differential conductance vs V for device Ni#1 with one Ni electrode, and (b) for device Co#1 with one Co electrode. Magnetic fields are applied to cause Zeeman splitting of the spin-up and spin-down resonances.

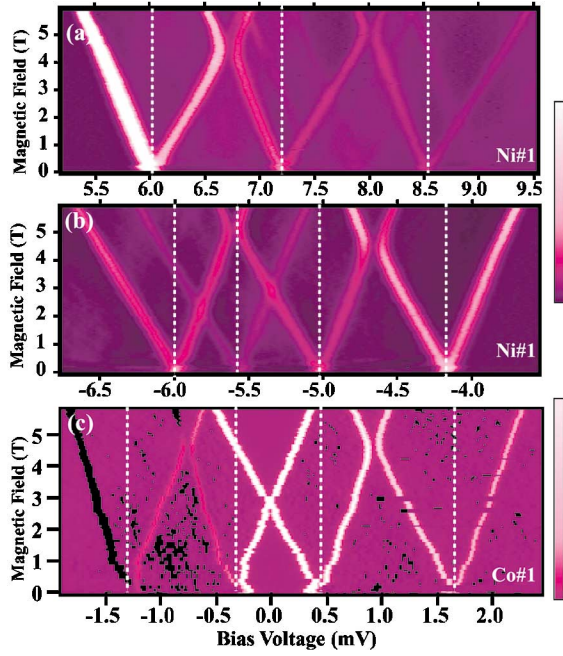


FIG. 2 (color online). dI/dV vs voltage and magnetic field for (a,b) device Ni#1 and (c) Co#1. The scales extend from 0 to (a,b) $0.2 \mu\text{S}$ and (c) $2 \mu\text{S}$. White indicates dI/dV values beyond the scale maximum, and in (c) black indicates negative values.

capacitances. The capacitance ratio can be determined by comparing the voltage for tunneling through the same state at positive and negative V [5]. We must also understand whether a resonance corresponds to a threshold for an electron tunneling on or off the particle, and across which tunnel junction. The transitions which correspond to tunneling between the particle and the Al electrode can be identified by the presence of a shift in their V positions as the Al electrode is driven from superconducting to normal by a magnetic field, and by the effect of the superconducting density of states (DOS) on the resonance shape [5]. The sign of V then determines whether an electron is tunneling on or off the particle. For the sample (Ni#1) shown in Figs. 1(a), 2(a), and 2(b), the transitions at positive V correspond to tunneling first from the dot to the Al electrode, with $eC_F/(C_N + C_F) = (0.42 \pm 0.02)e$. For the sample (Co#1) in Figs. 1(b) and 2(c), at positive V electrons are initially tunneling from the Co electrode to the particle, and $eC_N/(C_N + C_F) = (0.44 \pm 0.01)e$.

We will now analyze how the currents carried by individual states allow measurements of spin-dependent tunneling rates. The resistances of our tunnel junctions are sufficiently large (at least $1 \text{ M}\Omega \gg h/e^2$) that transport can be modeled by sequential tunneling [14,15]. The analysis takes a particularly simple form when the offset charge [14] has a value that permits tunneling at a low value of V so that only a single orbital state on the quantum dot contributes to current flow near the tunneling threshold [15,16]. This is the case for sample Co#1; the thresholds for more complicated nonequilibrium

tunneling processes, involving the lowest-energy even-electron excited state [9], are $V < -5.8 \text{ mV}$ or $V > 4.2 \text{ mV}$ at $B = 0$ in this sample. In general, the simple equilibrium tunneling regime can be achieved for any nanoparticle device made with a gate electrode so that the offset charge can be adjusted [16]. In Fig. 3(a), we show the I - V curve for sample Co#1 with $B = 1 \text{ T}$ to Zeeman split the resonances. The first step in current for either sign of V corresponds in this sample to an electron tunneling through only a spin-up (majority-spin) state. The sequential-tunneling theory [15] predicts that these two currents should have identical magnitudes,

$$I_{1+} = |I_{1-}| = e\gamma_1\gamma_N/(\gamma_1 + \gamma_N), \quad (1)$$

where γ_1 is the bare tunneling rate between the magnet and the spin-up state, and γ_N is the tunneling rate to the Al electrode. The fact that the steps do have the same magnitude confirms that electrons are tunneling via just one state. When $|V|$ is increased to permit tunneling through either the spin-up or spin-down state, the predicted values for the total current, using the methods in [14,15], are for positive and negative V ,

$$I_{2+} = \frac{e\gamma_N(\gamma_1 + \gamma_l)}{\gamma_N + \gamma_1 + \gamma_l}, \quad (2)$$

$$|I_{2-}| = \frac{2e\gamma_N}{1 + \gamma_N/\gamma_1 + \gamma_N/\gamma_l}. \quad (3)$$

We have made use of time-reversal symmetry which requires that the tunneling rates from the nonmagnetic electrode to both Zeeman-split states should be the same. This has been verified in a previous experiment [16]. We have also neglected spin relaxation based on experimental limits of relaxation rates slower than $5 \times 10^7 \text{ s}^{-1}$ in Al particles with Al electrodes [16], much slower than the tunneling rates. Equations (1)–(3) can be inverted to determine γ_N , γ_1 , and γ_l from I_{1+} , I_{2+} , and I_{2-} [Fig. 3(c)]. The resulting tunneling polarization, $(\gamma_1 - \gamma_l)/(\gamma_1 + \gamma_l)$, is positive [Fig. 3(d)], meaning that the tunneling rate for spin-up (majority) electrons in the ferromagnet is faster than for spin-down. This sign agrees with results for tunneling from ferromagnets through Al_2O_3 into thin-film superconducting Al [10,17], although the sign is opposite to the polarization of the DOS at the Fermi level within band-structure calculations [18]. This is understood to be due to much larger tunneling matrix elements for predominantly sp -band majority-spin electrons compared to predominantly d -band minority electrons, so that the matrix elements dominate over the DOS effect in determining the relative tunneling rates [19,20]. The magnitude of the tunneling polarization that we measure (8%–12%) is considerably less than the values 35%–42% found for Co using planar $\text{Co}/\text{Al}_2\text{O}_3/\text{Al}$ devices [10,17], and we observe some field dependence not seen in larger samples [Fig. 3(d)]. Both effects may indicate imperfections in our tunnel barriers; they have not undergone the process of optimization

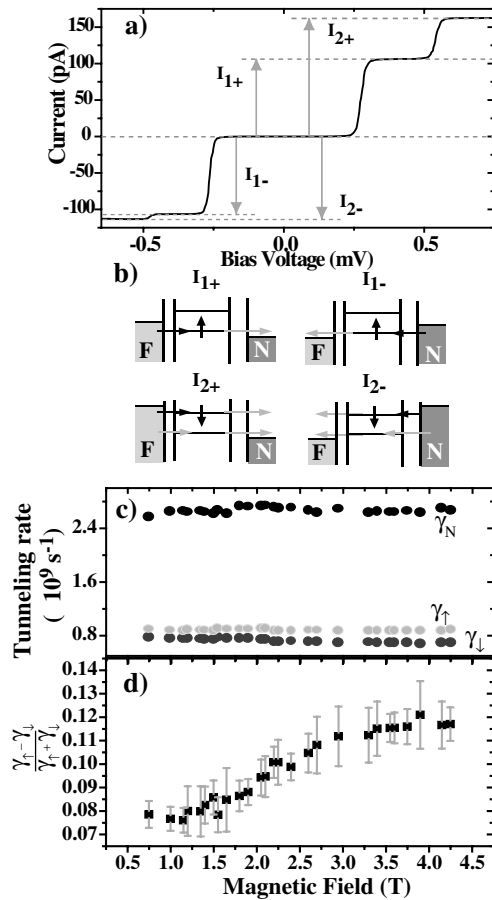


FIG. 3. (a) Current vs voltage curve for device Co# 1 for $B = 1$ T, showing the range of V where tunneling occurs via one pair of Zeeman-split energy levels. (b) Energy-level diagrams at each current step. Black horizontal arrows show the threshold tunneling transition. Gray arrows depict other transitions which contribute to the current. (c) The tunneling rates γ_{\uparrow} , γ_{\downarrow} , and γ_N were determined as described in the text. (d) Tunneling polarization for device Co#1.

which achieved large polarizations in larger-area devices [21]. The presence of any oxidation at the magnetic interface can reduce the tunneling polarization [21]. Our barriers are also very thin (with resistance-area products less than $200 \Omega \mu\text{m}^2$ compared to 10^7 – $10^{10} \Omega \mu\text{m}^2$ in most prior experiments [10,22]), which might reduce the polarization by increasing the relative tunneling rate of d states [23]. (However, recent work on optimized large-area $F/\text{Al}_2\text{O}_3/F$ tunnel junctions with $RA \sim 100 \Omega \mu\text{m}^2$ does not show reduced polarization [22].) We have considered whether the magnetic electrode might enhance spin relaxation within the particle so that it should not be neglected. This cannot explain the full reduction in our polarization; treating the relaxation rate as a free parameter, the maximum polarization consistent with the current steps in Fig. 3(a) is 21%.

In Figs. 1(b) and 2(c) at negative V , some higher-energy spin-down resonances produce signals with $dI/dV < 0$, meaning that they decrease the total current. This is a

consequence of the slower rate of tunneling for minority-spin electrons; an electron in the spin-down state blocks current flow through the spin-up channel until the electron tunnels slowly to the F electrode. By incorporating additional states into the sequential-tunneling model, we find a tunneling polarization of $15 \pm 6\%$ for the second Zeeman pair in sample Co#1.

Let us now consider the V positions of the tunneling resonances as a function of B . The magnitude of the Zeeman splitting is similar to previous measurements in all-Al devices [5]. After converting from V to energy as described above, we determine the g factor according to $\Delta E_{\text{Zeeman}} = g\mu_B B$. For the levels in Ni#1, g is between 1.83 ± 0.05 and 1.90 ± 0.07 , in Co#1 between 1.98 ± 0.07 and 2.05 ± 0.06 , and in the other devices discussed in this paper, $1.9 \leq g \leq 2.0$. However, the data in Fig. 2 differ from studies with nonmagnetic electrodes [5,16] in that the slopes of the spin-up and spin-down Zeeman shifts are not symmetric about 0; in Figs. 2(a) and 2(b), the midpoints of the Zeeman-split states tend to higher $|V|$ as a function of B , and in Fig. 2(c) they tend to lower values of $|V|$. This effect is expected in single-electron transistors (SETs) made with magnetic components, as a result of a field-dependent change in a magnet's electrochemical potential [11,13]. A related shift has been observed in micron-scale Ni/Co/Ni, Co/Ni/Co, and Al/Co/Al SETs [11]. When a magnetic field is applied to any bulk metal, it will flip some electron spins to align with B . Because a ferromagnet has different densities of states at the Fermi level for majority- and minority-spin states, the electrochemical potential must shift with B to accommodate the flipped spins. The magnitude of the shift will also be enhanced by exchange interactions in the magnet [13]. We will parametrize the shift by the variable $S = \Delta E_F(B)/\mu_B B$. When a magnet is incorporated as one electrode in an otherwise nonmagnetic SET, the experimental consequences of this shift are equivalent to a change in the energy of all the states in the nanoparticle by the amount $dE/dB = -\mu_B S C_F / (C_N + C_F)$ [11]. This analysis assumes that the magnetic field does not induce any rearrangements of charge density (see below).

Within each sample, the average slopes of the different Zeeman-split pairs correspond to the same value of S within measurement uncertainty. For the data in Figs. 2(a) and 2(b), the average slopes are $(2.6 \pm 0.2) \times 10^{-2}$ mV/T for positive V and $(1.85 \pm 0.2) \times 10^{-2}$ mV/T for negative V , giving in both cases $S = 0.45 \pm 0.04$. For noninteracting electrons with different majority and minority densities of states per unit energy at the Fermi level, ρ_{\uparrow} and ρ_{\downarrow} , the DOS polarization would give a shift $S = -(1/2)g[(\rho_{\uparrow} - \rho_{\downarrow})/(\rho_{\uparrow} + \rho_{\downarrow})]$, where g is the g factor [11,13]. Therefore a positive sign for S corresponds to a greater density of minority-spin states at the Fermi level, in agreement with band-structure calculations for Ni and Co [18]. However, the magnitude of the measured shift is surprisingly small. Band-structure

calculations for Ni give $\rho_{\downarrow}/\rho_{\uparrow} = 8.5$ [18], so that one would expect $S > 0.79$. We write this as a lower limit, because exchange interactions should increase S relative to predictions for noninteracting electrons [13]. For two other devices with a Ni electrode, made by the same procedure, we find even more striking discrepancies: $S = 0.15 \pm 0.1$ and 0.2 ± 0.1 . For three samples with a Co electrode, for which band-structure calculations suggest that $S > 0.59$ [18], we observe $S = 0.1 \pm 0.1$, 0.37 ± 0.05 (for Co#1), and 0.7 ± 0.1 . The existence of significant sample-to-sample variations is counter to expectations that the electrochemical shift should be a bulk property of the magnet [11,13].

We propose that the explanation of these discrepancies in the value of S is that a magnetic field may produce rearrangements in the charge distribution at a magnetic interface, which will modify the electric field in the tunnel junction and thus shift the energy levels of the nanoparticle as a function of B . In fact, such an effect should be expected within the same picture of wave functions that explains why majority-spin electrons are dominant in the tunneling polarization even though minority electrons have a larger density of states at the Fermi level. At an interface between Co or Ni and Al_2O_3 , the predominantly sp -band majority states have a longer decay length into the tunnel barrier than the d -band minority states [23]. Consequently, when an applied magnetic field transfers electrons from minority to majority states, some charge density at the surface of the magnet should shift slightly toward the barrier region [24]. The sign of the effect should cause the measured values of S to decrease for Ni and Co electrodes, and the magnitude can be computed simply from the work that the moving charge will do on an electron in the particle. Making the approximation that the spin-dependent densities at the magnet's surface are similar to the bulk, the charge density per unit area which changes spin at the last monolayer of the magnet is $\sigma \approx ea\rho_{\uparrow}\rho_{\downarrow}g\mu_B B/(\rho_{\uparrow} + \rho_{\downarrow})$, where a is the lattice constant. If the average position for charges in the minority and majority states differs by Δx at the surface layer, then this charge movement should alter the measured electrochemical shift by

$$\Delta S \approx -\frac{e^2}{\epsilon_0} ga(\Delta x) \frac{\rho_{\uparrow}\rho_{\downarrow}}{\rho_{\uparrow} + \rho_{\downarrow}} \quad (4)$$

$$\approx -12\Delta x/\text{\AA} \quad (5)$$

for either a Co or a Ni electrode. Therefore even in micron-scale devices [11], Δx as small as 0.01 \AA may decrease S by 10%, and foil attempts to measure the DOS polarization. In our devices, which have possibly nonuniform tunnel barriers, variations in Δx by less than 0.05 \AA can explain the sample-to-sample differences.

In summary, we have shown how individual Zeeman-split energy levels can be used to make quantitative measurements of tunneling polarization. This technique can serve as an alternative to the method of Meservey and

Tedrow [10], and allows the new capability of measuring this polarization locally, on the nanometer scale. We have also proposed that differences between spin-up and spin-down wave functions at magnetic interfaces may lead to spatial charge redistributions as a function of magnetic field. This effect will act to shift electronic energy levels in any spintronic device employing magnetic components.

We thank R. A. Buhrman, A. Champagne, S. Guéron, A. H. MacDonald, D. J. Monsma, and E. B. Myers for discussions. Funding was provided by ARO (DAAD19-01-1-0541), the Packard Foundation, and NSF (DMR-0071631 and use of the Cornell Nanofabrication Facility/NNUN).

-
- [1] P. L. McEuen *et al.*, Phys. Rev. Lett. **66**, 1926 (1991).
 - [2] S. Tarucha *et al.*, Phys. Rev. Lett. **77**, 3613 (1996).
 - [3] D. R. Stewart *et al.*, Science **278**, 1784 (1998).
 - [4] M. Ciorga *et al.*, Phys. Rev. B **61**, R16315 (2000).
 - [5] D. C. Ralph, C. T. Black, and M. Tinkham, Phys. Rev. Lett. **74**, 3241 (1995).
 - [6] J. R. Petta and D. C. Ralph, Phys. Rev. Lett. **87**, 266801 (2001).
 - [7] D. H. Cobden *et al.*, Phys. Rev. Lett. **81**, 681 (1998).
 - [8] S. Guéron, M. M. Deshmukh, E. B. Myers, and D. C. Ralph, Phys. Rev. Lett. **83**, 4148 (1999); M. M. Deshmukh *et al.*, Phys. Rev. Lett. **87**, 226801 (2001).
 - [9] P. Recher, E. V. Sukhorukov, and D. Loss, Phys. Rev. Lett. **85**, 1962 (2000).
 - [10] R. Meservey and P. M. Tedrow, Phys. Rep. **238**, 173 (1994).
 - [11] K. Ono, H. Shimada, and Y. Ootuka, J. Phys. Soc. Jpn. **66**, 1261 (1997); **67**, 2852 (1998).
 - [12] Magnitudes of the electrochemical shifts in Ref. [11] appear to be determined only to within about a factor of 2, due to uncertainties in Coulomb charging energies.
 - [13] A. H. MacDonald, in *Proceedings of the XVI Sitges Conference on Statistical Mechanics* (Springer-Verlag, Berlin, 2000), p. 211.
 - [14] J. von Delft and D. C. Ralph, Phys. Rep. **345**, 61 (2001).
 - [15] E. Bonet, M. M. Deshmukh, and D. C. Ralph, Phys. Rev. B **65**, 045317 (2002).
 - [16] M. M. Deshmukh, E. Bonet, A. N. Pasupathy, and D. C. Ralph, Phys. Rev. B **65**, 073301 (2002).
 - [17] D. J. Monsma and S. S. P. Parkin, Appl. Phys. Lett. **77**, 720 (2000).
 - [18] D. A. Papaconstantopoulos, *Handbook of the Band-Structure of Elemental Solids* (Plenum, New York, 1986).
 - [19] M. B. Stearns, J. Magn. Mater. **5**, 167 (1977).
 - [20] E. Y. Tsymlal and D. G. Pettifor, J. Phys. Condens. Matter **9**, L411 (1997).
 - [21] L. Seve *et al.*, Europhys. Lett. **55**, 439 (2001).
 - [22] D. J. Monsma and S. S. P. Parkin (unpublished).
 - [23] I. I. Oleinik, E. Y. Tsymlal, and D. G. Pettifor, Phys. Rev. B **62**, 3952 (2000).
 - [24] A related effect has been considered by S. Zhang, Phys. Rev. Lett. **83**, 640 (1999).